ELSEVIER

FEBS Letters 338 (1994) 227–233

FEBS LETTERS

FEBS 13605

Structural implications for the role of the N terminus in the 'superactivation' of collagenases

A crystallographic study

Peter Reinemer[a,*], Frank Grams[a], Robert Huber[a], Thomas Kleine[b], Susanne Schnierer[b], Michael Piper[b], Harald Tschesche[b], Wolfram Bode[a,*]

[a]*Max-Planck-Institut für Biochemie, Abteilung für Strukturforschung, D-82152 Martinsried, Germany*
[b]*Universität Bielefeld, Fakultät für Chemie und Biochemie, D-33615 Bielefeld, Germany*

Received 21 December 1993

Abstract

For the collagenases PMNL-CL and FIB-CL, the presence of the N-terminal Phe^{79} correlates with an increase in proteolytic activity. We have determined the X-ray crystal structure of the recombinant Phe^{79}–Gly^{242} catalytic domain of human neutrophil collagenase (PMNL-CL, MMP-8) using the recently solved model of the Met^{80}–Gly^{242} form for phasing and subsequently refined it to a final crystalographic *R*-factor of 18.0% at 2.5 Å resolution. The PMNL-CL catalytic domain is a spherical molecule with a flat active site cleft separating a smaller C-terminal subdomain from a bigger N-terminal domain, that harbours two zinc ions, namely a 'structural' and a 'catalytic' zinc, and two calcium ions. The N-terminal segment prior to Pro^{86}, which is disordered in the Met^{80}–Gly^{242} form, packs against a concave hydrophobic surface made by the C-terminal helix. The N-terminal Phe^{79} ammonium group makes a salt link with the side chain carboxylate group of the strictly conserved Asp^{232}. Stabilization of the catalytic site might be conferred via strong hydrogen bonds made by the adjacent, likewise strictly conserved Asp^{233} with the characteristic 'Met-turn', which forms the base of the active site residues.

Key words: Matrix metalloproteinase; Collagenase; Zinc endopeptidase family; X-ray crystal structure; Superactivation

1. Introduction

Matrix metalloproteinases are a family of zinc- and calcium-dependent endopeptidases that exhibitit proteolytic activities towards most of the constituents of the extracellular matrix, such as the interstitial and basement membranes, fibronectin or laminin. Due to their central role in extracellular matrix degradation, they have been implicated in tissue remodelling processes associated with mammalian growth and development and in various pathological conditions such as rheumatoid arthritis or tumor invasion [1–3]. At least nine distinct, but highly homologous family members have been identified, including the collagenase subfamily comprising the interstitial collagenase (FIB-CL, MMP-1) and the neutrophil collagenase (PMNL-CL, MMP-8). Each member consits of an amino-terminal propeptide (maintaining latency), a catalytic domain harbouring the zinc- and calcium-sites, and a C-terminal hemopexin like domain, which is important for the unique ability of FIB-CL and PMNL-CL to cleave collagen [3–7].

In contrast to the FIB pro-CL, which is secreted immediately after synthesis [8], PMNL pro-CL is stored as a highly glycosylated protein within specific granules of neutrophils and can be secreted as an inactive precursor after initiation by inflammatory mediators [9–11]. Conversion of the latent proenzyme to the active enzyme is a crucial step in the neutrophil-mediated initiation of collagenolysis during inflammatory connective tissue turnover. In vitro, activation cleavage initiated by proteinases, mercurials or oxidants leads in a stepwise process to finally active species having either Phe^{79}, Met^{80} (Val^{80} in case of FIB-CL) or Leu^{81} as the N-terminal residue [10,12–16]. Activation with stromelysin-1 (SL, MMP-3) gives rise to a 'superactivated' enzyme, which exhibits a significantly higher activity than either of the two other forms; different activation factors have been reported including an approximately 4- to 12-fold activity for N-terminal Phe^{79} FIB-CL [14,17–18] and approx-

*Corresponding authors.

Abbreviations: MMP, matrix metalloproteinases; PMNL, polymorphonuclear leucocytes; FIB, fibroblast; CL, collagenase; Tris, Tris(hydroxymethyl)aminomethane; MES, 2-morpholinoethane sulfonic acid; PEG, polyethylenglycol.

SSDI 0014-5793(93)E1522-N

imately 3.5-fold activity for N-terminal Phe[79] PMNL-CL [16], respectively. It has been shown, that the predominant species upon stromelysin activation is the Phe[79] form, demonstrating that 'superactivity' is linked with this form [14,16]. The structural basis of this phenomenon has been unclear until now. Recently, we described the X-ray crystal structure of Met[80]–Gly[242] catalytic domain of human PMNL-CL [19] at 2.0 Å resolution. In this structure the N-terminal hexapeptide Met[80]-Leu-Thr-Pro-Gly-Asn[85] was disordered; electron density was only observed from Pro[86] onwards. Here we present the 2.5 Å X-ray crystal structure of Phe[79]–Gly[242] catalytic domain of human PMNL-CL, where the N terminus is well ordered, and discuss the phenomenon of 'superactivation' in the light of this structure.

2. Experimental

2.1. Purification of the N-terminal Phe[79] catalytic domain of human PMNL-CL

A C-terminally truncated short form of PMNL-CL lacking the hemopexin-like domain was expressed in *E. coli* and refolded as previously described [5]. The latent, C-terminally truncated enzyme was activated by addition of active, recombinant Stromelysin-1 to a final concentration of 0.2 μM and incubated at 37° C for 16 h. The activated enzyme, i.e. the catalytic domain of PMNL-CL (Phe[79]–Gly[242]), was afterwards purified to homogeneity by hydroxamate affinity chromatography [5]. The identity of the N-terminal Phe[79] was confirmed by amino-terminal sequence determination.

2.2. Crystallization

Hanging droplets were made by mixing 1.5 μl protein solution (~12 mg/ml protein in 5 mM $CaCl_2$, 100 mM NaCl, 3 mM MES/NaOH, 0.02% NaN_3, pH 6.0), 2 μl inhibitor solution (50 mM Pro-Leu-Gly-NHOH [20]) and 6 μl PEG- solution (10% (m/v) PEG 6000, 0.2 M MES/NaOH, 0.02% NaN_3, pH 6.0). PMNL-CL catalytic domain was crystallized by vapour diffusion at 22°C against 1 M potassium phosphate buffer, 0.02% NaN_3, pH 6.0. Small crystals of approximately 0.5 × 0.06 × 0.03 mm were obtained within 3 days. They were harvested into 20% (m/v) PEG 6000, 500 mM NaCl, 100 mM $CaCl_2$, 0.1 M MES/NaOH, 0.02% NaN_3, pH 6.0 and diffract to at least 2.5 Å resolution. The crystals belong to the orthorhombic space group $P2_12_12_1$ having the lattice constants $a = 33.21$, $b = 69.53$, $c = 72.54$ Å, $\alpha = \beta = \gamma = 90°$. The asymmetric unit contains a monomer.

2.3. Structure analysis

X-ray measurements were done on a MAR image plate area detector (MAR Research, Hamburg) mounted on a Rigaku rotating anode X-ray generator ($\lambda = 1.5418$ Å, operated at 5.4 kW). X-ray intensities were evaluated with the MOSFLM program package [21] and loaded to the PROTEIN program package [22]. Data collection statistics are given in Table 1. A 2 F_o–F_c electron density map was calculated using the model the of Met[80]–GLy[242] form of PMNL-CL [19] for phasing. The N-terminal sequence Phe[79]-Met-Leu-Thr-Pro-Gly-Asn[85] [23] was unambiguously defined in the electron density map and was incorporated using the interactive graphics program FRODO [24]. The model was subjected to reciprocal space least squares refinement with energy constraints as implemented in X-PLOR [25] using force field parameters derived by Engh and Huber [26]. The final refinement statistics are shown in Table 2.

3. Results

The X-ray crystal structure of the Phe[79]–Gly[242] catalytic domain of human PMNL-CL in complex with the inhibitor Pro-Leu-Gly-NHOH has been solved at 2.5 Å resolution using the Met[80]–Gly[242] form for phasing and subsequently refined to convergence at a final crystallographic R-factor of 18.0% using all data ($I > 0\ \sigma(I)$) from 8.0 to 2.5 Å resolution. The overall structure of the Phe[79]–Gly[242] form as well as inhibitor binding are almost identical to that of the Met[80]–Gly[242] form, which has been previously described in detail [19]. For the reader's convenience we will briefly summarize the main aspects; the catalytic domain of human PMNL-CL consists of an N-terminal main domain and a C-terminal small domain separated by a relatively flat active-site cleft (as shown in Fig. 1). The main domain comprises a central, highly twisted five-stranded β-sheet, flanked by an S-shaped double loop and two other bridging loops on its convex side and by two long α-helices on its concave side, respectively (for secondary structure elements see Table 3). It

Fig. 1. Structure of the Phe[79]–Gly[242] catalytic domain of human PMNL-collagenase shown as a ribbon model (using the program RIBBON [31]; modified by A. Karshikoff). An upper (N-terminal) and a lower (C-terminal) domain are separated by a moderately deep-active site cleft. The upper domain harbours two zinc ions (displayed as spheres with the coordinating ligands), the 'structural' zinc (Zn^{998}, on the top, coordinated by three histidines and an aspartate) and the 'catalytic' zinc (Zn^{999}, in the middle, coordinated by three histidines and the inhibitor's hydroxamic moiety (thick lines)), and two calcium ions (Ka^{996}, Ka^{997}, displayed as spheres without coordinating ligands).

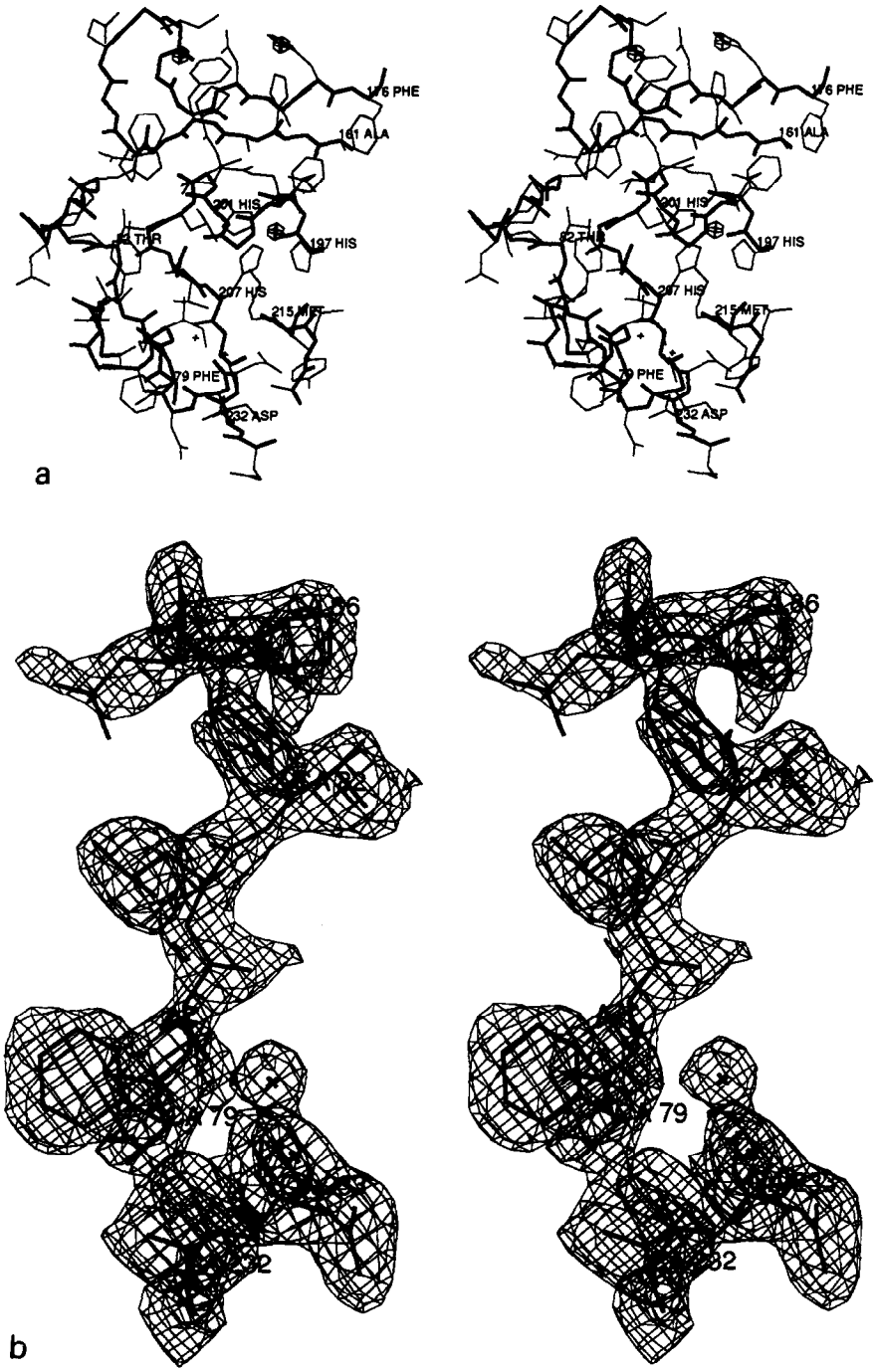

Fig. 2 (a) Detailed model of the N terminus of Phe^{79}–Gly^{242} catalytic domain of human PMNL-collagenase including the N terminus (Phe^{79}–Trp^{88}), β-strand 4 and 5 (Ala^{161}–Phe^{176}), the active site helix αB and the extended element follwing αB which contains the third zinc-liganding His^{207} (His^{197}–Ser^{208}), the 'Met-turn' (Ala^{213}–Tyr^{216}), the 'catalytic' zinc ion (displayed as a sphere), the inhibitor H_2N-Pro-Leu-Gly-NHOH, and the C-terminal helix αC (Gln^{231}–Gly^{242}). (b) Final $2F_o$–F_c electron density map of the N terminus with the model of the residues Phe^{79}–Pro^{86}, Asp^{232}–Asp^{233}, and two solvent molecules overlayed. The contour level is 1.0 σ.

harbours two zinc ions, referred to hereafter as the 'catalytic' zinc (Zn^{999}), and the extremely tight bound 'structural' zinc ion (Zn^{998}), and two calcium ions (Ka^{996}, Ka^{997}). The 'catalytic' zinc is situated at the bottom of the active-site cleft and is coordinated by the three His-residues of the His^{197}-Glu^{198}-X-X-His^{201}-X-X-Gly^{204}-X-X-His^{207} zinc-binding consensus sequence and by the inhibitor's hydroxamic acid moiety. The 'structural' zinc ion and Ka^{997} are sandwiched between the surface S-shaped double loop and the surface of the β-sheet; Zn^{998} is tetrahedrally coordinated by His^{147}, Asp^{149}, His^{162} and His^{175}, while Ka^{997} is octahedrally coordinated by Asp^{154}, Gly^{155}, Asn^{157}, Ile^{159}, Asp^{177}, and Glu^{180}. The second calcium ion is located on the convex side of the β-sheet at the end of

Table 1
Statistics of data collection

Number of measurements	20139
Number of observations	19447
Number of unique reflections ($I > 0\ \sigma(I)$)	5804
Completeness of data (%)	
∞–2.50 Å	93.5
2.56–2.50 Å	84.1
R_{Merge} [1]	0.125
R_{Sym} [2]	0.072

[1] $R_{Merge} = \Sigma_h\Sigma_i\ (|I(h,i) - < I(h) > |)/\Sigma_h\Sigma_i\ I(h,i)$, where $I(h,i)$ is the intensity value of the i-th measurement of h and $< I(h) >$ is the corresponding mean value of h for all i measurements of h: the summation is over all measurements

[2] $R_{Sym} = \Sigma\ (|I_F - < I_F > |)/\Sigma\ I_F$, where I_F is the averaged value of point group related reflections and $< I_F >$ is the averaged value of a Bijvoet pair

Table 2
Final refinement statistics

Resolution range (Å)	8.0–2.5
Number of unique data in resolution range	5683
Total number of protein atoms (excluding H)	1317
Solvent atoms (excluding H)	108
R-factor[1]	
8.0–2.5 Å	0.180
2.55–2.50 Å	0.233
Root-mean-square deviations from target values	
Bonds (Å)	0.012
Angles (°)	1.7

[1] $R = (\Sigma|F_o - F_c|)/\Sigma F_o$

a glycine-rich open loop and is also octahedrally coordinated by Asp[137], Gly[169], Gly[171], Asp[173], and by two solvent molecules. The small C-terminal domain exhibits a largely irregular folding, with a wide right-handed loop followed by an α-helix. The loop is stabilized by a tight 1,4-turn Ala[213]-Leu-Met-Tyr[216] known as the 'Met-turn' [27–28], a conserved topological element in the 'metzinkins' [28] providing a hydrophobic base for the 'catalytic' zinc ion and the three His residues.

The inhibitor lies antiparallel to the edge strand (β4), with Pro[I1] residing in a hydrophobic groove formed by the side chains of His[162], Phe[164] and Ser[151]; Leu[I2] forms two inter-main chain hydrogen bonds to Ala[163], and its side chain is situated in a small opening lined by His[201], Ala[206] and His [207], while Gly-NHOH[I3] is oriented towards Glu[198] with the carbonyl oxygen and the hydroxyl oxygen complexing the 'catalytic' zinc (see Figs. 1 and 2a).

A remarkable feature in the structure of Met[80]–Gly[242] catalytic domain of human PMNL-CL is the concave surface at the bottom of the molecule, located between Pro[86] and Ser[209] and formed by the C-terminal helix αC and the strand following helix αB. The structure of the Phe[79]-variant reveals that the N-terminal heptapeptide segement Phe[79]-Met-Leu-Thr-Pro-Gly-Asn[85] binds to this region (see Fig. 2a for model and Fig. 2b for electron density map). The N terminus extends backwards from the N-terminal residue of β1 (Asn[92]) in a loop towards the active site cleft with the side chain of Trp[88] slotting into a hydrophobic groove formed by the side chains of Leu[93] (β1), Ile[138] (β3), Pro[166], Gly[172] (both situated in the loop connecting β4 to β5) and Leu[203] (situated at the C-terminal end of αB), respectively, thereby stabilizing the loop. It extends to Pro[86] which is situated near Gly[204], i.e. next to the active-site helix αB (left to αB in Figs. 1 and 2a). The chain adopts a 1,4-tight turn Thr[82]-Pro-Gly-Asn[85], with the side chain of Thr[82] fitting into a small hydrophobic groove lined by Pro[86], Gln[165], Gly[204] and Ala[206] and pointing towards the inhibitor's Leu (I2) moiety. N-terminal to Thr[82] the chain turns downward to the C-terminal helix αC, crossing over with the strand following helix αB at residue Leu[205] to form the only regular inter main chain hydrogen bond. The N-terminal ammonium group (of Phe[79]) forms a salt bridge with the carboxylate moiety of the strictly conserved residue Asp[232] (Fig. 2a,b). The side chains of Leu[81] and Phe[79] are oriented towards the C-terminal helix with the former packing against the side chains of Ile[240] (αC) and Asn[85] and the latter packing against Gly[236] (which is strictly conserved) and Ala[239] of the C-terminal helix αC, while the side chain of Met[80] points towards the bulk solvent and seems to be disordered, as no significant electron density could be observed for this residue. Interestingly, the N terminus locks two water molecules in a cavity, which is created by the C-terminal helix and the strand following the active-site helix and lined by the side chains of Val[205], Trp[120], Met[215], Asp[232], Asp[233] and Gly[236], respectively. Both internal solvent molecules are hydrogen bonded to Asp[233] $O_{\delta 1}$ and to Met[80] NH (Fig. 2a,b).

4. Discussion

Activation studies of latent pro-FIB-CL and pro-PMNL-CL show that species activated with stromelysin-

→

Fig. 3. Truncated C_α-representations of Astacin [29–30] (top), the catalytic domain of human PMNL-collagenase (middle), and Adamalysin II [27] (bottom) showing the structure of the N terminus and the main structure elements creating its environment (β1, β3, β4, β5, the elements containing the 'catalytic' zinc signature, the C-terminal helix αC, and the 'catalytic' zinc ions with their liganding histidines). The N-terminal structures (Astacin: completely buried; PMNL-CL: packed but not buried; Adamalysin II: freely exposed) are related to their role in the enzymatic active species (see section 4 for details).

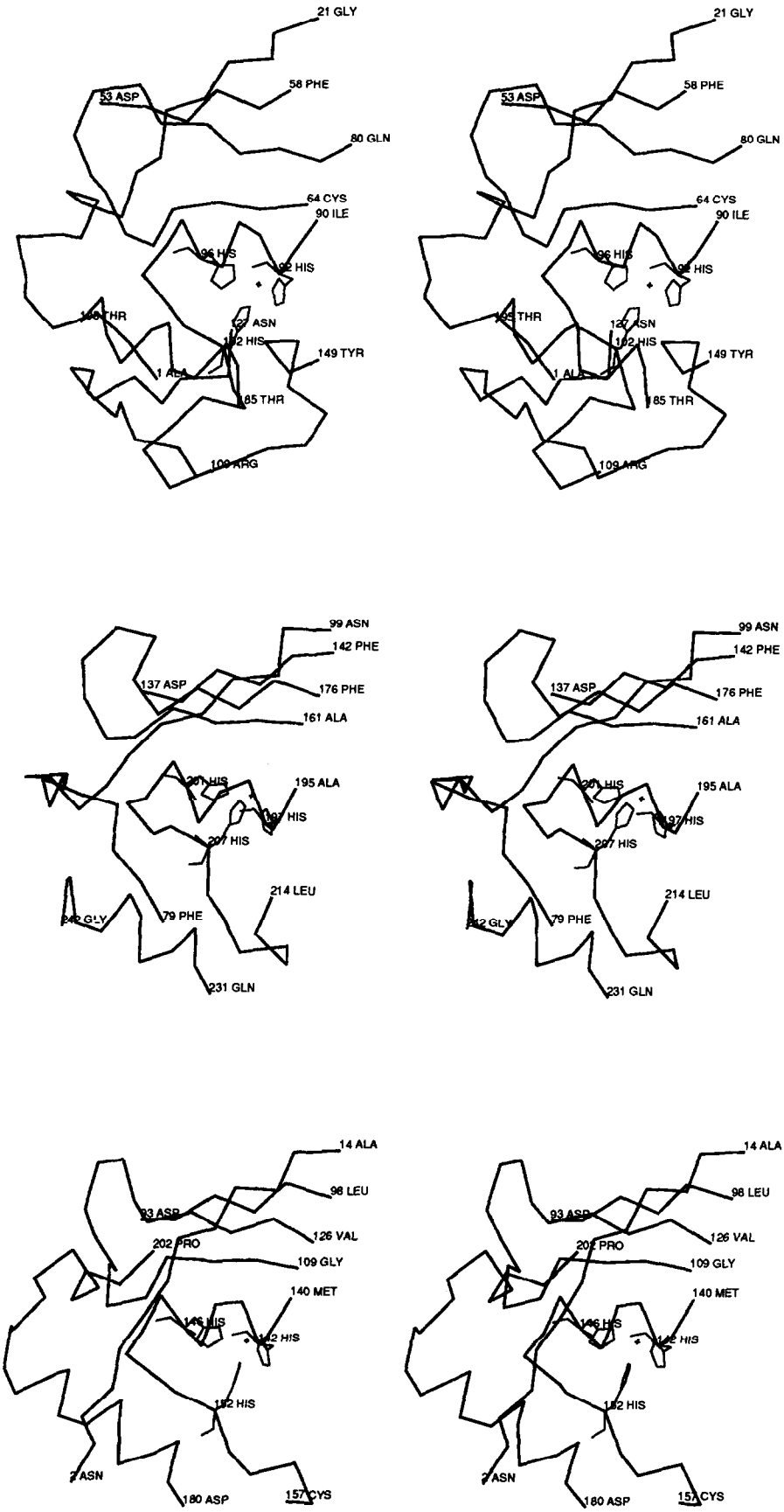
21 GLY
58 PHE
53 ASP
80 GLN
64 CYS
90 ILE
96 HIS
92 HIS
106 THR
124 ASN
92 HIS
149 TYR
1 ALA
185 THR
109 ARG
21 GLY
58 PHE
53 ASP
80 GLN
64 CYS
90 ILE
96 HIS
92 HIS
106 THR
124 ASN
92 HIS
149 TYR
1 ALA
185 THR
109 ARG
99 ASN
142 PHE
137 ASP
176 PHE
161 ALA
207 HIS
195 ALA
197 HIS
207 HIS
214 LEU
79 PHE
231 GLN
99 ASN
142 PHE
137 ASP
176 PHE
161 ALA
207 HIS
195 ALA
197 HIS
207 HIS
214 LEU
79 PHE
231 GLN
14 ALA
98 LEU
93 ASP
126 VAL
202 PRO
109 GLY
140 MET
146 HIS
142 HIS
152 HIS
2 ASN
180 ASP
157 CYS
14 ALA
98 LEU
93 ASP
126 VAL
202 PRO
109 GLY
140 MET
146 HIS
142 HIS
152 HIS
2 ASN
180 ASP
157 CYS

1 have a significantly higher proteolytic activity than species activated by other procedures [14,16–18]. However, although significant, the activity differences are rather small. Using collagen as substrate activity enhancement factors of about 12 [17], 5–8 [18] and 4–6.5 [14] have been derived for full-length FIB-CL. For full-length PMNL-CL they are approximately 2 and 3.5 using a synthetic octapeptide and collagen as substrate, respectively [16]. This phenomenon has been termed 'superactivation' [3], and it has been demonstrated that it is only observed with species having Phe^{79} as N-terminal residue of the active form [14,16–18].

A superposition of the structural models of the Phe^{79}–Gly^{242} form and of the Met^{80}–Gly^{242} form of human PMNL-CL (not shown, rms-deviation is 0.178 Å for all atoms) reveals that both molecules superimpose well and that, in particular, the geometry of the active-site residues remains unchanged. As expected from the moderate observed enhancement factors, the 'superactivation' would not seem to be related to (or caused by) a visible structural reorientation in the active site. The significant disorder–order transition of the N-terminal segment must in some way be linked to activity enhancement. The formation of the salt-link between the N-terminal ammonium group and the side chain of Asp^{232} seems to be the main triggering effect on the active site, requiring an N terminus of correct length (including residue 79).

The two structures (i.e. the Phe^{79}–Gly^{242} and the Met^{80}–Gly^{242} catalytic domain) show no obvious differences in position and rigidity of the active-site residues; dynamic aspects beyond the accuracy of the models may nevertheless be important. The differences might reside in very tiny structural (motional) differences leading to stabilization of the active site and hence of the transition states. Alternatively, the reduced activity of N-terminally truncated forms could be caused by interference of the mobile N-terminal segment with a peptide substrate to be bound.

These findings are in good agreement with the results of the activity studies mentioned above, and explain that Asp^{232} is strictly conserved in collagenases [3]. Another strictly conserved residue is Gly^{236}, positioned one turn away from Asp^{232} in the C-terminal helix. This residue serves as a contact site for the side chain of residue 79 (which is in almost every case aromatic, i.e. Phe or Tyr [3]). Any other amino acid replacing it would cause stereochemical strain by its side chain protruding towards the aromatic side chain of Phe^{79}, most probably preventing the correct orientation of the N terminus.

Fig. 3 shows the main secondary structure elements together with the N-terminal segements for PMNL-CL, astacin [29–30] and adamalysin II [27], the latter serving as examples for two other important subfamilies of the 'metzinkins' [28]. It is interesting to compare the N-terminal structures and relate them to the role of the N terminus for activation of the latent proenzyme. In

Table 3
Secondary structure elements of the catalytic domain of human PMNL-CL [32]

Structural element	Residues
β1	92–97
αA	106–121
β2	127–130
β3	138–143
β4	160–163
β5	174–177
αB	191–202
αC	231–240

PMNL-CL (Fig. 3, middle) the N terminus packs against the C-terminal helix and the extended chain element Gly^{204}–Ser^{209}, i.e. the N terminus is packed but not buried. In astacin (Fig. 3, top) the N terminus is arranged in a topologically similar manner but is completely buried in a groove shielded from the bulk solvent by a wide loop element extending from Asn^{127} to Tyr^{149}. The ammonium group of its N-terminal residue (Ala^1) forms a solvent mediated salt bridge to Glu^{103}, the residue that immediately follows the third zinc-liganding histidine. Interestingly, while the position of the N terminus is somewhat similar to that in PMNL-CL, the position of the C-terminal helix is considerably shifted. This is quite different from the situation in adamalysin II (Fig. 3, bottom), where the N terminus is much shorter and is freely exposed, while the C-terminal helix is positioned quite similar to that in PMNL-CL, even though the C terminus extends much further and reaches up to the β-sheet.

Thus, the collagenases occupy an intermediate position between the astacins and the adamalysins with respect to the orientation of the N terminus: in the astacins the N terminus is entirely buried, while it is packed but not buried in the collagenases and freely exposed in the adamalysins. This relates to the role of the N terminus in the enzymatic active species. In the astacins an active conformation would seem to require a precisely processed N terminus; N-terminally elongated molecules presumably adopt a different (and possibly inactive) conformation. For the collagenases, it has been demonstrated that the correct processing of the N terminus is not essential but nevertheless important for maximal enzymatic activity. Finally, for the adamalysins it is quite clear that the N terminus most likely has no effect on the enzymatic activity.

Acknowledgements: We are grateful to Dr. M.T. Stubbs for helpful discussions. The financial support of Bayer AG (PF-F/Biotechnology, Monheim, Germany) to P.R., of the SFB 223 of the Universität Bielefeld to T.K. and H.T., of the Fonds der Chemischen Industrie to H.T., of the SFB 207 of the Universität München and of the Fonds der Chemischen Industrie to W.B. is gratefully acknowledged.

References

[1] Woessner, J.F. (1991) FASEB J. 5, 2145–2154.
[2] Matrisian, L.M. (1992) Bio Essays 14, 455–463.
[3] Birkedal-Hansen, H., Moore, W.G.I., Bodden, M.K., Windsor, L.J., Birkedal-Hansen, B., DeCarlo, A. and Engler, J.A. (1993) Crit. Rev. Oral Biol. Med. 4, 197–250.
[4] Hasty, K.A., Jeffrey, J.J., Hibbs, M.S. and Welgus, H.G. (1987) J. Biol. Chem. 262, 10048–10052.
[5] Schnierer, S., Kleine, T. Gote, T., Hillemann, A., Knäuper, V. and Tschesche, H. (1993) Biochem. Biophys. Res. Commun. 191, 319–326.
[6] Knäuper, V., Osthues, A., DeClerk, Y.A., Langley, K.A., Bläser, J. and Tschesche, H. (1993) Biochem. J. 291, 847–854.
[7] Sanchez-Lopez, R., Alexander, C.M., Behrendtsen, O., Breathnach, R. and Werb, Z. (1993) J. Biol. Chem. 268, 7238–7247.
[8] Nagase, H., Brinckerhoff, C.E., Vater, C.A. and Harris, E.D. (1983) Biochem. J. 214, 281–288.
[9] Murphy, G., Reynolds, J.J., Bretz, U. and Baggiolini, M. (1977) Biochem. J. 162, 195–197.
[10] Knäuper, V. Krämer, S., Reinke, H. and Tschesche, H. (1990) Eur. J. Biochem. 189, 295–300.
[11] Hasty, K.A., Hibbs, M.S., Kang, A.H. and Mainardi, C.L. (1986) J. Biol. Chem. 261, 5645–5650.
[12] Grant, G.A., Eisen, A.Z., Marmer, B.L., Roswit, W.T. and Goldberg, G.I. (1987) J. Biol. Chem. 262, 5886–5889.
[13] Mallya, S.K., Mookhtiar, K.A., Gao, Y., Brew, K., Dioszegi, M., Birkedal-Hansen, H. and van Wart, H.E. (1990) Biochemistry 29, 10628–10634.
[14] Suzuki, K., Engfield, J.J., Morodomi, T., Salvesen, G. and Nagase, H. (1990) Biochemistry 29, 10261–10270.
[15] Bläser, J., Knäuper, V. Osthues, A., Reinke, H. and Tschesche, H. (1991) Eur. J. Biochem. 202, 1223–1230.
[16] Knäuper, V., Wilhelm, S.M., Seperack, P.K., DeClerk, Y.A., Langley, K.E., Osthues, A. and Tschesche, H. (1993) Biochem. J. 295, 581–586.
[17] Murphy, G., Cockett, M.I., Stephens, P.E., Smith, B.J. and Docherty, A.J.P. (1987) Biochem. J. 248, 265–268.
[18] He, C., Wilhelm, S.M., Pentland, A.P., Marmer, B.L., Grant, G.A., Eisen, A.Z. and Goldberg, G.I. (1989) Proc. Natl. Acad. Sci. USA 86, 2632 –2636.
[19] Bode, W., Reinemer, P., Huber, R., Kleine, T., Schnierer, S. and Tschesche, H. (1994) EMBO J., in press.
[20] Moore, W.M. and Spilburg, C.A. (1986) Biochemistry 25, 5189–5195.
[21] Leslie, A.G.W. (1991) Daresbury Lab. Inf. Quart Prog. Crystallogr. 26 (available from the Librarian, SERC Laboratory, Daresbury, Warrington, WA4 4AD, UK).
[22] Steigemann, W. (1991) in: From Chemistry to Biology (Moras, D., Podjarny, A.D. and Thierry, J.C., Eds.) Crystallographic Computing vol. 5, pp. 115–125, Oxford University Press, Oxford, UK.
[23] Hasty, K.A., Pourmotabbed, T.F., Goldberg, G.I., Thompson, J.P., Spinella, D.G., Stevens, R.M. and Mainardi, C.L. (1990) J. Biol. Chem. 265, 11421–11424.
[24] Jones, T.A. (1978) J. Appl. Crystallogr. 15, 23–31.
[25] Brünger, A.T., Karplus, M. and Petsko, G.A. (1989) Acta Cryst. Sect. A 45, 50–61.
[26] Engh, R.A. and Huber, R. (1991) Acta Cryst. Sect. A 47, 392–400.
[27] Gomis-Rüth, F.-X., Kress, L.F. and Bode, W. (1993) EMBO J. 12, 4151–4157.
[28] Bode, W., Gomis-Rüth, F.-X. and Stöcker, W. (1993) FEBS Lett., 331, 134–140.
[29] Bode, W., Gomis-Rüth, F.X., Huber, R., Zwilling, R. and Stöcker, W. (1992) Nature 358, 164–167.
[30] Gomis-Rüth, F.X., Stöcker, W., Huber, R., Zwilling, R. and Bode, W. (1993) J. Mol. Biol. 229, 945–968.
[31] Priestle, J.P. (1988) J. Appl. Crystallogr. 21, 572–576.
[32] Kabsch, W. and Sander, C. (1983) Biopolymers 22, 2577–2637.